

Article

Multivariate Evaluation of Photovoltaic Utilization Potential of Primary and Secondary School Buildings: A Case Study in Hainan Province, China

Chaohong Wang ^{1,2,3}, Xudong Zhang ¹ , Wang Chen ⁴, Feihu Jiang ¹ and Xiaogang Zhao ^{1,2,3,*}

- ¹ School of Architecture and Art Design, Hebei University of Technology, Tianjin 300130, China; wangchaohong@hebut.edu.cn (C.W.); xudongzhang0129@163.com (X.Z.); jfh18822041079@163.com (F.J.)
- ² Key Laboratory of Healthy Human Settlements in Hebei Province, Tianjin 300130, China
- ³ Urban and Rural Renewal and Architectural Heritage Protection Center, Hebei University of Technology, Tianjin 300132, China
- ⁴ Tropical Building Science Research Institute (Hainan) Co., Ltd., Haikou 570100, China; chenwang@cabr.com.cn
- * Correspondence: zhaoxiaogang@hebut.edu.cn

Abstract: Modernization and industrialization have significantly increased energy consumption, causing environmental problems. Given that China is the largest energy user, the rise in building energy consumption necessitates clean energy alternatives. The purpose of this study is to summarize typical building models for primary and secondary schools in Hainan Province, and to use software to simulate and calculate the photovoltaic utilization potential of primary and secondary school buildings. In China, the government is usually the manager of primary and secondary schools, and due to their architectural characteristics, these buildings can be used to assess photovoltaic applications. The aim is to drive the application of photovoltaic systems in all types of buildings and promote urban energy reform. This study summarizes the types of primary and secondary school buildings in Hainan Province and analyzes them. It evaluates rooftop photovoltaic projects at the Second Middle School and the Siyuan School in Wanning City, Hainan Province, and uses PVsyst 7.2 software to assess the photovoltaic utilization potential. The results show that the optimal orientation in Hainan Province is south-facing, and the optimal inclination angle is 10° to 20°. The most favorable orientations of facade photovoltaic systems are 20° southeast or southwest. The longest dynamic investment payback period is approximately 15 years, and the environmental benefits are \$0.012/kWh. The findings indicate significant potential for photovoltaic applications in primary and secondary school buildings. A combination of facade and rooftop photovoltaics can result in the zero-energy consumption of these buildings, reducing the pressure on urban power grids and achieving sustainable utilization.

Keywords: solar energy; energy balance; zero energy building; building-attached photovoltaics; analysis of photovoltaic potential



Citation: Wang, C.; Zhang, X.; Chen, W.; Jiang, F.; Zhao, X. Multivariate Evaluation of Photovoltaic Utilization Potential of Primary and Secondary School Buildings: A Case Study in Hainan Province, China. *Buildings* **2024**, *14*, 810. <https://doi.org/10.3390/buildings14030810>

Academic Editors: Hazim B. Awbi and Eusébio Z.E. Conceição

Received: 1 December 2023

Revised: 1 March 2024

Accepted: 6 March 2024

Published: 16 March 2024



Copyright: © 2024 by the authors. Licensee MDPI, Basel, Switzerland. This article is an open access article distributed under the terms and conditions of the Creative Commons Attribution (CC BY) license (<https://creativecommons.org/licenses/by/4.0/>).

1. Introduction

The world must reduce greenhouse gas emissions to zero within approximately 30 years to limit global warming to 1.5 °C based on the Paris Agreement. Most countries must achieve carbon neutrality by 2050. As the world's largest CO₂ emitter, China has significant responsibilities in global energy conservation and emission reduction efforts. Therefore, studying China's energy conservation and emission reduction efforts is required to achieve the zero-carbon goal. In 2020, the Chinese government proposed the goals of peaking carbon emissions by 2030 and achieving carbon neutrality by 2060.

Energy consumption is steadily increasing in China due to urbanization. Building energy consumption accounts for about 30% of the total energy consumption. According

to the experience of developed countries, building energy consumption is expected to increase to about 35%. NPC and CPPCC have proposed that China's building coverage area exceeds 73 billion square meters, of which at least 95% are covered by high-energy consuming buildings that do not meet energy-saving standards. Therefore, it is urgent to find feasible strategies to reduce energy consumption and improve the energy structure of existing buildings while meeting the needs of urban construction. In addition to improving energy savings, renewable energy should be considered for existing buildings.

According to the Annual Development Report on Building Energy Efficiency in China, the energy consumption used for the construction and operation of buildings in China accounted for 32% of the total energy consumption in 2020, which is close to the global proportion. However, construction energy accounts for 11% of the total energy consumption, which is higher than the global proportion of 6%. The energy consumption of building operations accounts for 21% of the total energy consumption, lower than the global average level [1]. The proportion of building energy consumption will continue to increase due to China's urbanization and improved living standards. The proportion of CO₂ emissions in China's building construction and operation in 2020 accounted for 32% of the total CO₂ emissions, with building construction and operation accounting for 13% and 19%, respectively. The proportion of energy consumption and CO₂ emissions is detailed in Figure 1.

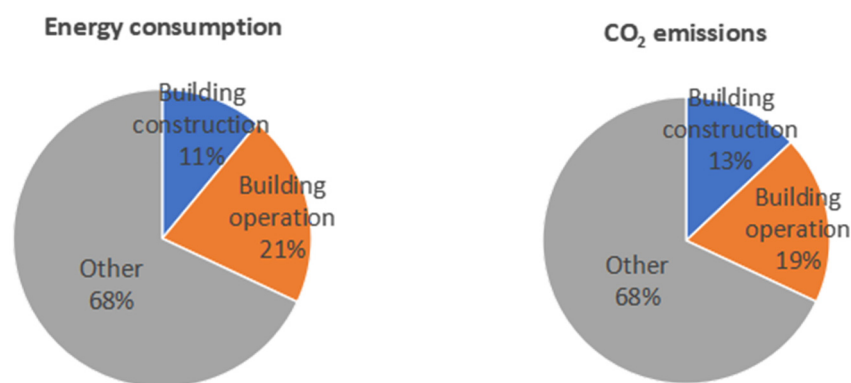


Figure 1. Energy consumption and CO₂ emissions in building construction and operation.

New energy technologies, such as facade photovoltaic power generation, are effective in reducing building carbon emissions. China has excellent solar radiation resources; over two-thirds of the country's area has an annual sunshine duration exceeding 2200 h and an annual total solar radiation exceeding 5000 MJ/m², making it highly suitable for building photovoltaic applications. Many studies have analyzed the potential for building photovoltaic utilization in various countries. Hu, M J et al. [2] developed a rapid and accurate rooftop extraction method using object-based image classification, the normalized difference vegetation index (NDVI), and digital surface models (DSMs). The results were used to identify suitable rooftops for solar panel installation. Ranjgar, B et al. [3] estimated the rooftop solar power production potential in Tehran, the capital city of Iran, using a Geographic Information System (GIS) to assess big data on building parcels. Zhao K M et al. [4] identified five building prototypes in Adelaide and quantified the solar energy potential of building facades for different urban forms. Singh D et al. [5] analyzed the potential and losses of applying three PV cell technologies (Crystal Silicon, Copper indium diselenide, Cadmium Telluride) in different climate regions of India. In addition, some scholars have analyzed the impact of factors such as the air gap, ventilation rate and tilt angle of PV shading devices, adjacent shading, semitransparent PV (STPV) glazing design, cell coverage ratio (CCR), transmittance, window to wall ratio (WWR), and glazing orientation on the power generation efficiency of building photovoltaic systems [6,7].

China's 14th Five Year Plan for Development states: "Promote the integrated design, construction, and installation of solar photovoltaic systems in new buildings, and

encourage government investment in public welfare buildings to strengthen the application of solar photovoltaic systems. The structural safety and fire safety of buildings or facilities equipped with solar photovoltaic systems should be ensured, and the potential for installing solar photovoltaic systems on building roofs, walls, ancillary facilities, and municipal public facilities should be evaluated." Many studies have been conducted to assess the potential for photovoltaic utilization in urban areas and neighborhoods in China, especially for different building types. Zhang, W J et al. [8] used GIS to calculate the rooftop area for photovoltaic systems in Chinese urban buildings and conducted an investment analysis of buildings with photovoltaic systems. Zhang H et al. [1] proposed an evaluation method for the potential utilization of rooftop solar energy in China's urban areas. They used GIS analysis to calculate the photovoltaic utilization potential of existing building roofs in the central urban area of Tianjin and future urban development. Wang Y et al. [9] conducted a comprehensive study on the power generation and cost-effectiveness ratio of photovoltaic systems installed in a large number of residential areas in Shanghai before the 1990s and summarized strategies for retrofitting photovoltaic systems in existing residential areas. Chen Y B et al. [10] utilized GIS databases and data from 270 meteorological stations in China to incorporate energy, economic, and environmental and evaluated the potential of distributed rooftop photovoltaics in various Chinese regions from a macro perspective. Xu W et al. [11] analyzed the photovoltaic system of the Baoshang Bank building and used Ecotect to establish an annual solar radiation model for building surfaces. They determined the optimal system configuration and constructed an evaluation model for the solar energy utilization potential of buildings from three dimensions: peak energy potential, economic potential, and social potential. Liu C P et al. [12] studied the potential of individual photovoltaic applications in residential buildings in different climate zones in China. They analyzed the power generation capacity under different climate conditions, building heights, photovoltaic inclination angles, orientations, photovoltaic conversion efficiencies, and other factors. From existing research, it has been found that the evaluation indicators for the potential utilization of building photovoltaics mainly include the physical potential [13–15], such as the amount of solar radiation received by the building surface; geographical potential [16–18], such as the resource conditions limited by the regional geographical location; technical potential [19,20], such as system power generation efficiency and performance; economic potential [21–23], such as investment costs and dynamic investment payback periods; and the environmental potential [24–26], such as the full life cycle power generation of photovoltaic systems converted into the amount of pollutants reduced by traditional electricity. Most research on building photovoltaic potential in China was conducted at the urban or community level, whereas few studies evaluated the potential of individual buildings and did not consider building energy consumption.

China is strongly promoting building photovoltaic systems [27]. However, few of these systems have been implemented in southern China, especially in Hainan Province. There is an urgent need for research to guide the development and implementation of building photovoltaics. Due to the government's usual management of primary and secondary school buildings and their energy use characteristics, these buildings can be used as models to investigate photovoltaic applications in various regions. Therefore, this study evaluates rooftop photovoltaic projects at the Second Middle School and Siyuan School in Wanning City, Hainan Province. The characteristics of typical primary and secondary school buildings in South China are summarized. Meteorological data from Hainan Province are used to conduct simulations using Ladybug tools 1.4.0 and PVsyst 7.2 software to assess the physical, technical, economic, and environmental benefit potential and production-demand balance of photovoltaic systems in primary and secondary school buildings. The results indicate the significant potential of building photovoltaics in primary and secondary school buildings to achieve zero carbon emissions. The findings can guide the conversion of conventional to photovoltaic energy generation and promote urban energy structure transformation to achieve China's carbon peak and carbon neutrality goals.

2. Methodology

This study first investigates the application of rooftop photovoltaics in primary and secondary school buildings in Hainan Province, collects monthly photovoltaic power generation data, and evaluates actual cases from multiple perspectives. Apply Ladybug and PVsyst software to simulate actual cases and compare and analyze them with actual situations to verify the accuracy of the software simulation. Through extensive case studies, summarize the typical spatial layout forms of primary and secondary school buildings in hot summer and warm winter areas of China, and determine the building form, window to wall ratio, and exterior skin area. Use Ladybug to simulate the external solar radiation of typical models and analyze the physical potential of photovoltaic applications in primary and secondary school buildings. Obtain the optimal tilt angle, azimuth angle, and array spacing through formula calculation and PVsyst simulation, and analyze their technical potential. The software simulates the annual power generation data of the building and compares it with the building's energy consumption to analyze its potential for balancing production and demand. Calculate the total investment and dynamic investment payback period, and analyze the economic and environmental potential of pollutant emission reduction through formulas. The method concepts used in this study are shown in Figure 2.

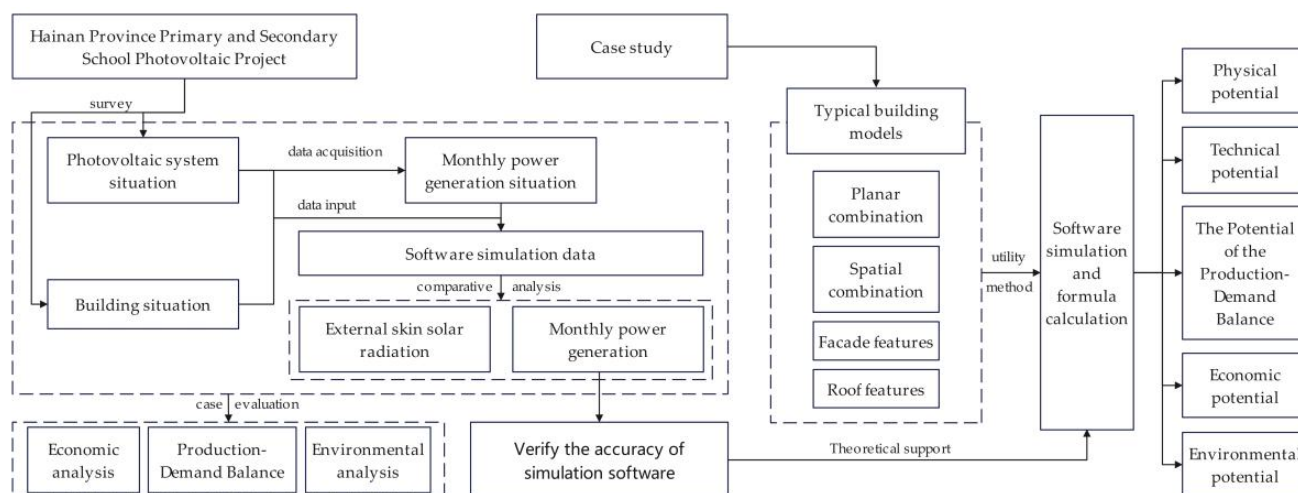


Figure 2. The main methods used in the article.

3. Analysis of Photovoltaic Systems in School Buildings in Hainan Province

3.1. Row-Type Building—Overview of the Photovoltaic System of the Second Middle School in Wanning City

The Wanning Second Middle School (hereafter referred to as School A) was the first “Roof Photovoltaic Leader” project in Wanning City. The project was completed and implemented in November 2021. The photovoltaic system of this project is located on the roofs of four buildings, with a roof area of 1885 m² and an installed capacity of 170.64 kW. The azimuth angle of this photovoltaic system is 3° southeast (fixed angle). The photovoltaic panels are tilted at an angle of 15° from the horizontal plane (Table 1) [28].

Table 1. Parameters of the Photovoltaic System of the Wanning Second Middle School.

Building Name	Number of Photovoltaic Modules	Installed Capacity	Photovoltaic Module Specifications	Inverter Configuration
Building 1	84	45.36 kW		
Building 2	76	41.04 kW	Size: 2274 × 1134 × 35 mm	20 kW × 1 unit
Building 3	50	27 kW	Peak power: 540 W	50 kW × 2 unit
Building 4	106	57.24 kW	Module efficiency: 20.94%	60 kW × 1 unit

3.2. Integrated Building—Overview of the Photovoltaic System of the Wanning Siyuan School

The photovoltaic system of the Wanning Siyuan School (hereafter referred to as School B) was implemented in October 2021. The roof area of the project is 4312 m², and 344 single crystal photovoltaic modules with a power of 540 Wp were installed. The total installed capacity is 185.76 kWp. The photovoltaic array is oriented in the same direction as the building, with an azimuth angle of 13° southeast and an installation angle of 10° (Table 2) [28].

Table 2. Parameters of the Photovoltaic System of the Siyuan School.

Building Name	Number of Photovoltaic Modules	Installed Capacity	Photovoltaic Module Specifications	Inverter Configuration
Building 5	108	58.32 kW		
Building 6	58	31.32 kW	Size: 2274 × 1134 × 35 mm Peak power: 540 W Module efficiency: 20.94%	30 kW × 1 unit
Building 7	66	35.64 kW		36 kW × 1 unit
Building 8	112	60.48 kW		60 kW × 2 unit

3.3. Analysis of the Balance between Production and Demand

The photovoltaic systems of School A and School B have been operating steadily since they were implemented. The annual power generation in 2022 is shown in Figure 3.

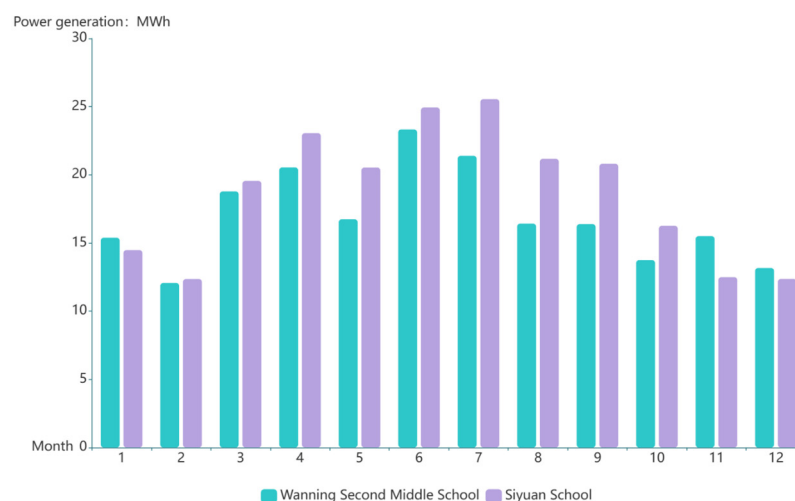


Figure 3. Measured monthly power generation of two photovoltaic systems.

The installed capacity of the two projects is similar, and the monthly power generation of the photovoltaic system exceeds 12 MWh. The photovoltaic power generation is lower in February due to fewer days. The annual power generation of School A is 205.47 MWh, and that of School B in Wanning City is 223.60 MWh. The photovoltaic system of School A generates more power in November, December, and January and has higher photoelectric conversion efficiency under unfavorable solar radiation conditions than that of School B because the photovoltaic inclination angle is closer to the optimal angle in Wanning City. Therefore, the annual power generation efficiency is higher for School A than for School B.

The total building area of each floor with photovoltaic systems of School A and School B are, respectively, 12135 m² and 19185 m². The requirement of the standard [29] is that the power consumption per unit building area of secondary education institutions in Haikou City is 30.4 kWh/(m²·a). Therefore, the average annual electricity consumption of the two photovoltaic buildings is 368.90 MWh and 583.22 MWh, respectively.

The annual power generation of the two photovoltaic buildings is lower than their annual average energy consumption, meeting a maximum of 54% of the annual energy consumption. Therefore, a balance between energy production and demand in

Hainan's primary and secondary school buildings cannot be achieved by relying solely on rooftop photovoltaic systems. Utilizing building facades to install photovoltaic systems can achieve this balance.

3.4. Economic Analysis of Photovoltaic Utilization

This study used the dynamic investment payback period as an evaluation indicator of the photovoltaic utilization efficiency. The dynamic investment payback period refers to the period when the net income of the system is equal to zero. It can be calculated as follows:

$$\sum_{t=0}^{P'_t} (C_i - C_0)_t (1 + i)^{-t} = 0 \quad (1)$$

where P'_t is the dynamic investment payback period; t is implementation year of the system; C_i represents the investment into the system, in dollars; C_0 represents the system's cost, in dollars; and i is the benchmark discount rate.

According to the data provided by the developer, the initial investment for the rooftop photovoltaic system of School A and School B was \$0.52/Wp. The total investment costs of the two projects were \$88,962.73 and \$96,845.50, respectively. The maintenance costs of the photovoltaic systems mainly include the regular cleaning of the photovoltaic panels and maintenance of the photovoltaic module and circuits. The maintenance cost in the first year of system construction and operation was 0.2% of the initial investment cost. The maintenance cost increased by 10% over the previous year, starting in year 2, because of additional maintenance costs and inflation. The electricity price of the Hainan Power Grid [30] for non-residential users is \$0.088/kWh. The benchmark discount rate used in this study is 8% of the capital return rate of the photovoltaic industry, considering the funding sources, investment opportunity costs, project risks, and inflation rate.

The dynamic investment payback period for the photovoltaic systems of School A and School B is 5.410 and 5.412 years. The rooftop photovoltaic systems of both projects have excellent economic performance, with a net income of \$311,084.54 and \$338,486.56, respectively, during the projects' life cycles, representing 3.5 times the investment cost.

3.5. Environmental Benefit Analysis

This study evaluated the environmental benefits of the rooftop photovoltaic systems of School A and School B by comparing the systems with a coal-fired thermal power generation system.

The total power generation of the rooftop photovoltaic systems of School A and School B during their 25-year life cycle is 5136.70 MWh and 5589.88 MWh, respectively. The National Energy Administration's report states that the average standard coal consumption of thermal power plants in 2021 was 302.5 g/kWh. Therefore, the rooftop photovoltaic systems of the two projects save 1553.85 and 1690.94 tons of standard coal during their life cycles, respectively. Table 3 lists the pollutant emissions from the combustion of 1 ton of standard coal and the environmental cost per unit pollutant.

Table 3. Unit emission reduction coefficient and environmental cost [31–33].

Pollutant	Pollutant Emission Rate/kg·t ⁻¹	Environmental Cost/Dollars·kg ⁻¹
CO ₂	1731	0.0032
SO ₂	22	0.83
NO _x	10	1.1
TSP	17	0.31

The environmental benefits of two schools were calculated based on the pollutant emissions generated by the combustion of 1 ton of standard coal and the environmental cost per unit pollutant, as shown in Table 4. Compared with coal-fired thermal power

generation, the total pollutant emission reduction of the rooftop photovoltaic systems of the two projects during their life cycle is 2765.85 kiloton and 3009.87 kiloton, respectively, resulting in an environmental benefit of \$0.012/kWh.

Table 4. Total emission reduction of pollutants and environmental benefits.

Project Name	Pollutant	Emission Reduction/t	Environmental Benefit/Dollars
School A	CO ₂	2689.71	8599.79
	SO ₂	34.19	28,512.59
	NO _x	15.54	17,280.36
	TSP	26.42	8078.57
	Total	2765.85	62,471.31
School B	CO ₂	2927.02	9358.51
	SO ₂	37.20	31,028.15
	NO _x	16.91	18,804.94
	TSP	28.75	8791.31
	Total	3009.87	67,982.91

3.6. Summary

The photovoltaic systems of the primary and secondary school buildings in Hainan Province exhibit excellent investment returns and environmental benefits. However, a gap exists between the energy consumption and production capacity of the primary and secondary school buildings when relying solely on rooftop photovoltaic systems. Establishing an integrated rooftop and facade photovoltaic system is critical to achieving a balance between energy consumption and production.

4. Analysis of Primary and Secondary School Building Types in Hainan Province

4.1. Analysis of Primary and Secondary School Building Types in Hainan Province

4.1.1. Room Configuration of School Buildings

The three primary functional spaces of primary and secondary school buildings are classrooms and other teaching spaces, and auxiliary spaces, such as offices, toilets, stairwells, and corridors. According to the requirements of "Code for design of school" [34], typical room sizes for the main functional rooms, such as classrooms, offices, toilets, and staircases, are shown in Figure 4.

4.1.2. Configuration of School Buildings

The common types of teaching buildings in primary and secondary schools in Hainan Province fall into two categories based on the design standards and the areas' climate characteristics: row-type and integrated buildings. Row-type buildings and their forms are composed of one or more long strips, and each row of buildings can be connected independently or through corridors. Integrated buildings typically consist of two or more rows of buildings, are connected by functional rooms rather than simple corridors, and typically appear in a rectangular-ambulatory-plane.

This study investigated 20 primary and secondary school buildings in hot summer and warm winter areas and summarized the classroom orientation, lighting methods, and corridor types. The results are illustrated in Table 5. Most primary and secondary school buildings had north-to-south orientations and a corridor on one side. Schools with a corridor on the south side and classrooms on the north side were the most common, accounting for 40%, followed by schools with an outer corridor on the north and classrooms on the south side (20%) and various types (40%).

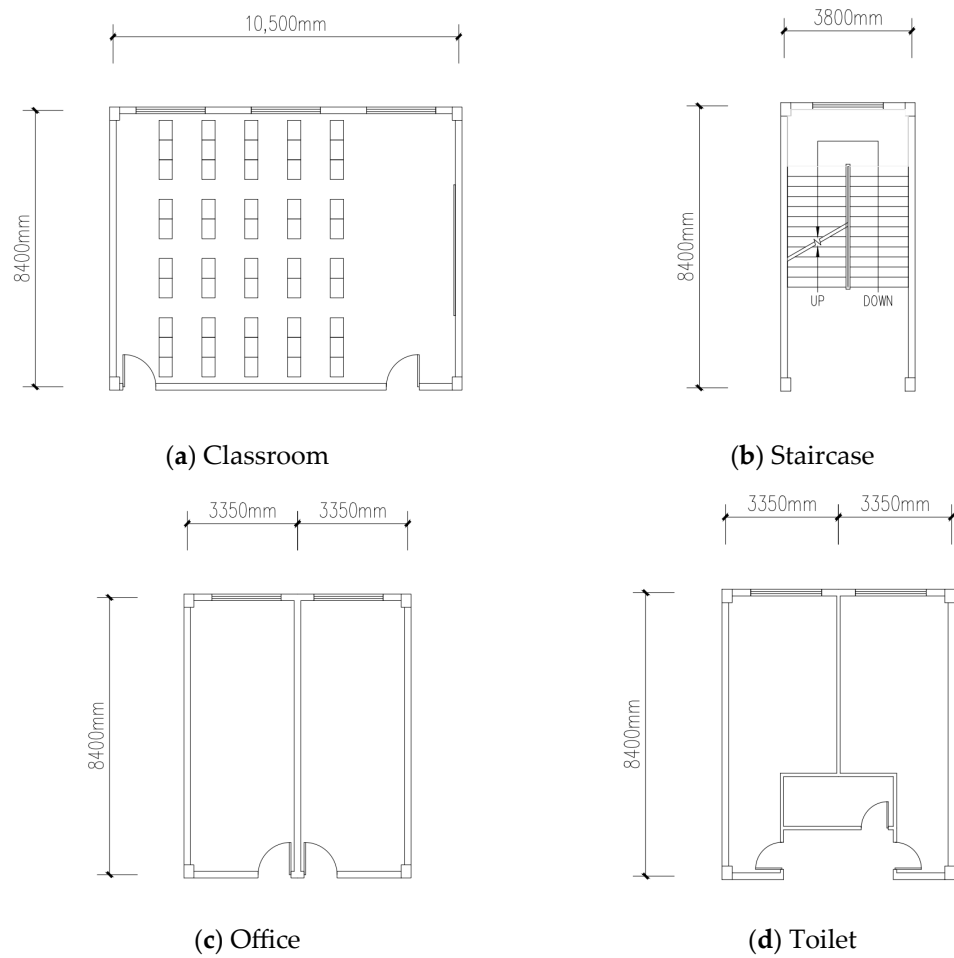


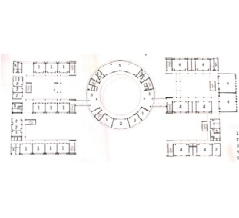
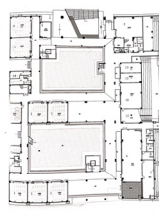
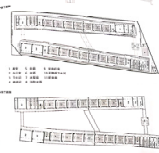
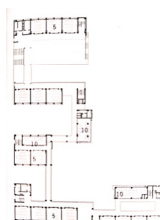
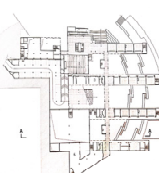
Figure 4. Typical floor plans of school rooms.

Table 5. The configuration of primary and secondary school buildings.

Corridor Type	Layout	
	Row-Type Building	Integrated Buildings
south outer corridor	4, 6, 7, 14	1, 8, 10, 19
north outer corridor	17, 18	9
south and north double outer corridors	15, 3	5
circular external corridor	12, 13	2, 11
middle corridor	16	20

1 2 3 4 5

Table 5. Cont.

Corridor Type	Layout	
	Row-Type Building	Integrated Buildings
		
6	7	8
		
9	10	11
		
12	13	14
		
15	16	17
		
18	19	20

The characteristics of Hainan primary and secondary school buildings can be summarized as follows:

- (1) The most common orientation of the buildings is north to south, and bilateral lighting is typical. Most primary schools have five floors, and most secondary schools have six floors.
- (2) Two configurations are prevalent: row-type and integrated buildings.

Based on previous research and actual conditions, the floor plans of the teaching buildings in primary and secondary schools in the Hainan region can be classified into four categories, as shown in Figure 5.

The standard [34] states that the number of floors in classrooms in primary schools cannot exceed four, and that in secondary schools cannot exceed five. However, many primary and secondary school buildings have five or six floors, respectively, due to high urban density. Our survey showed that most schools had five floors, with a height of 3.1 m. Four common configurations of teaching buildings in primary and secondary schools in Hainan Province are shown in Figure 6.

This article establishes a physical, technological, production-demand balance, economic, and environmental potential evaluation model for photovoltaic systems in primary and secondary schools in Hainan Province.

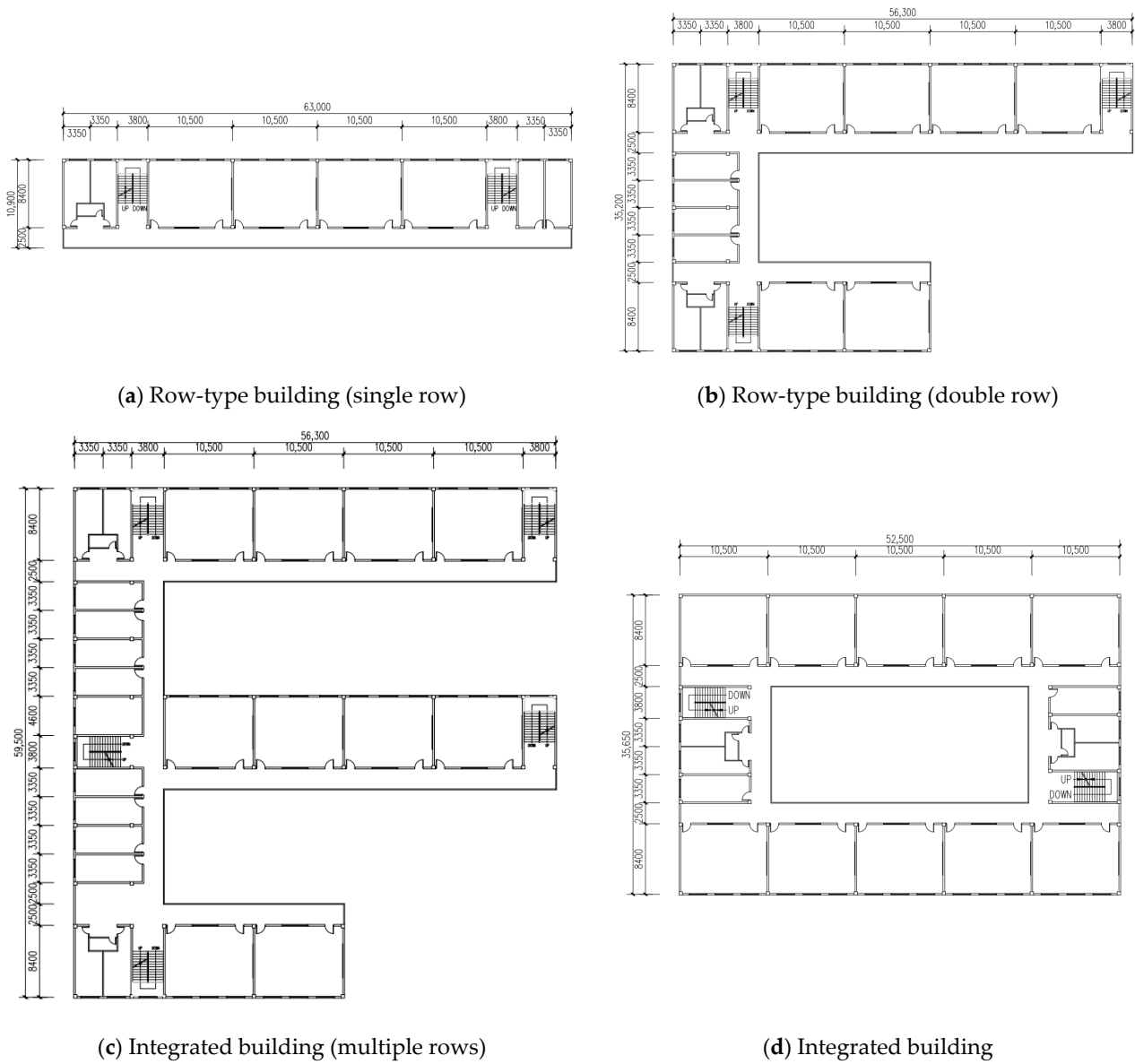
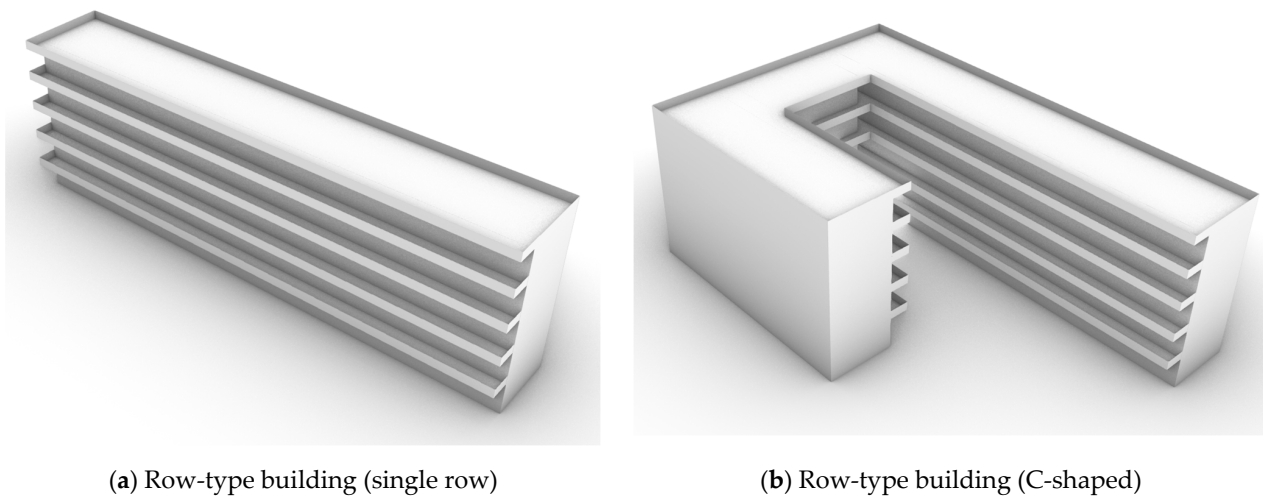


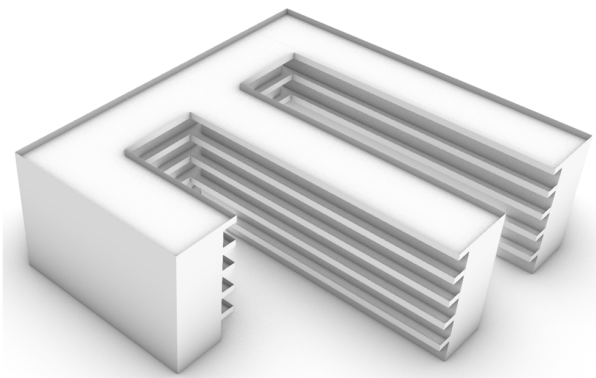
Figure 5. Typical floor plans of row-type and integrated buildings (mm).



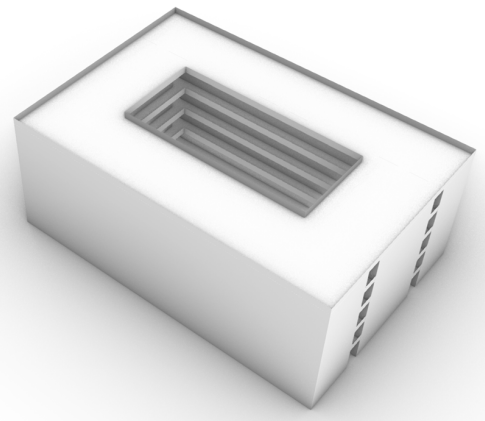
(a) Row-type building (single row)

(b) Row-type building (C-shaped)

Figure 6. Cont.



(c) Integrated building (multiple rows)

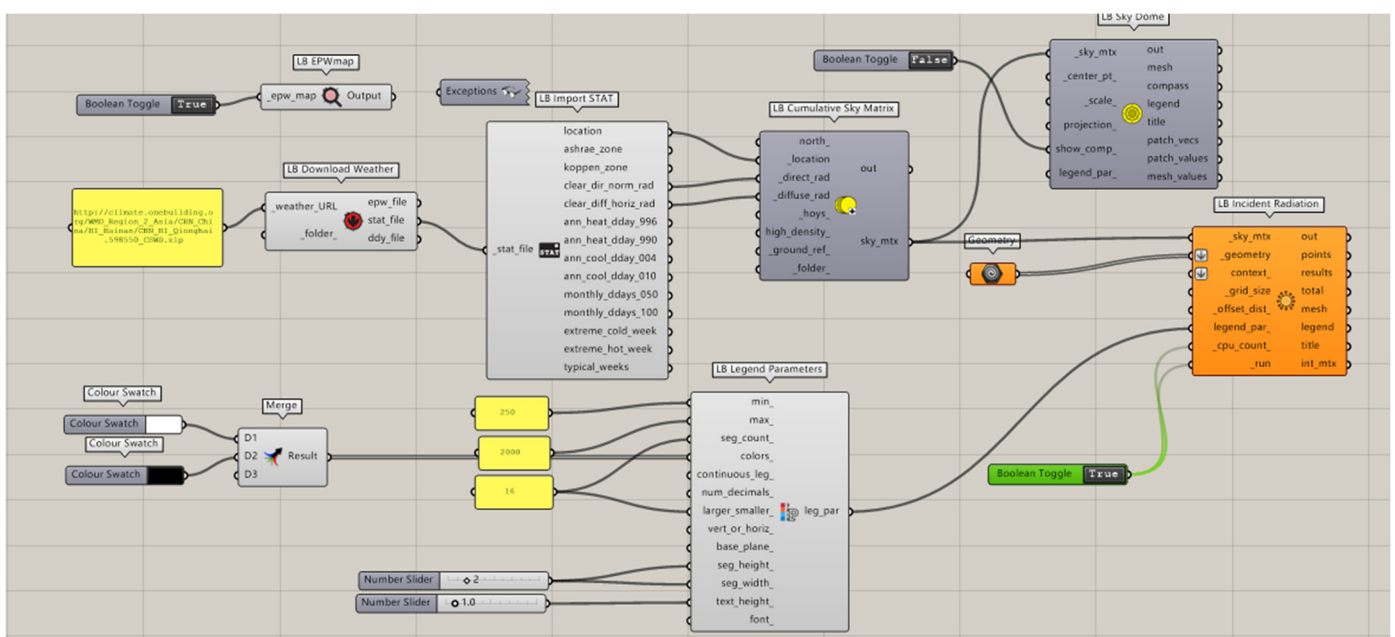


(d) Integrated building (open)

Figure 6. Typical model.

4.2. Simulation and Verification of Building Photovoltaic System Model

This study used School A as an example to assess the solar radiation on the building surfaces. The Ladybug software was used to simulate the annual solar radiation of the building envelope. The parameter module built in Ladybug software is shown in Figure 7, and the calculated solar radiation is shown in Figure 8.

**Figure 7.** Battery Block Configuration in Ladybug Software.

The solar radiation intensity on the roof is relatively high and stable, with an average solar radiation of 2.31 MWh/m^2 . Monocrystalline silicon photovoltaic modules with high power generation efficiency should be installed to improve the power generation capacity of photovoltaic systems and ensure that the system efficiency exceeds 80%. These solar panel types have been installed in School A.

PVsyst was used to simulate the power generation capacity of the photovoltaic system. A comparison of the measured and simulated power generation capacity is shown in Figure 9.

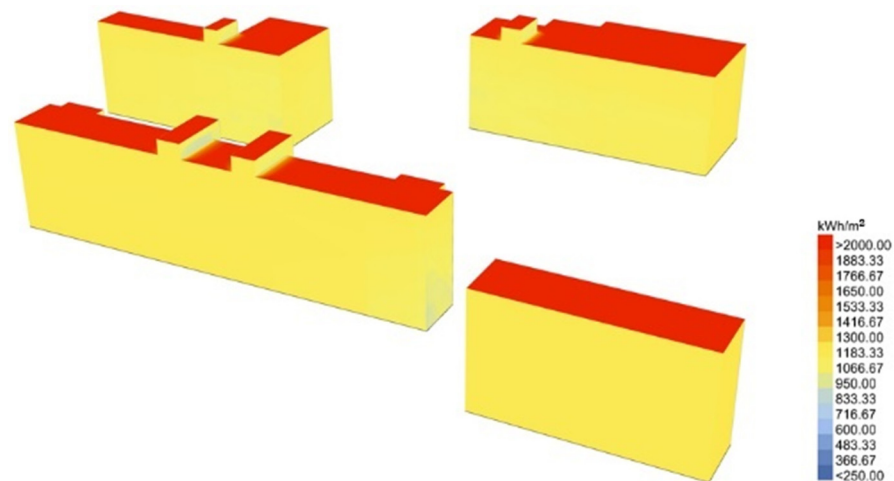


Figure 8. Solar radiation on building surfaces.

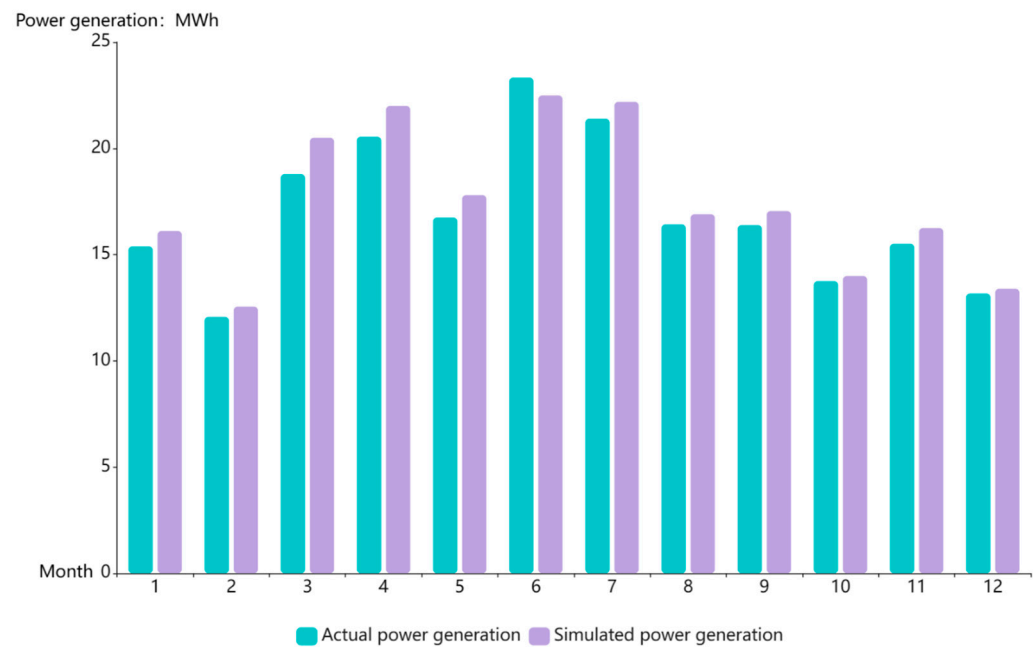


Figure 9. Comparison of simulated and measured power generation capacity of the photovoltaic system of School A.

The results indicate that the simulated and measured values are similar. The simulated power generation capacity is slightly higher, which is attributed to the influences of meteorological factors. However, the monthly average error is within 5%, indicating sufficient accuracy.

4.3. Physical Potential of the Photovoltaic System

The physical potential of the photovoltaic system refers to the total amount of solar energy reaching the target surface, i.e., the solar radiation intensity on the building surface. Meteorological data from the Hainan region were used to assess this aspect.

This study used Ladybug software and Chinese standard weather data (CSWD) from the Haikou area to simulate the annual solar radiation on the surface of the four building types (Figure 10). The companion standard was used to quantify the annual solar radiation. It has been used by many Chinese and international scholars to quantify the solar radiation potential of urban building walls and roofs for active and passive solar heating, photovoltaic power generation, and lighting [35]. The minimum annual solar radiation levels for the

exterior walls and roofs of buildings for solar power generation are 0.8 MWh/m^2 and 1.0 MWh/m^2 , respectively [36].

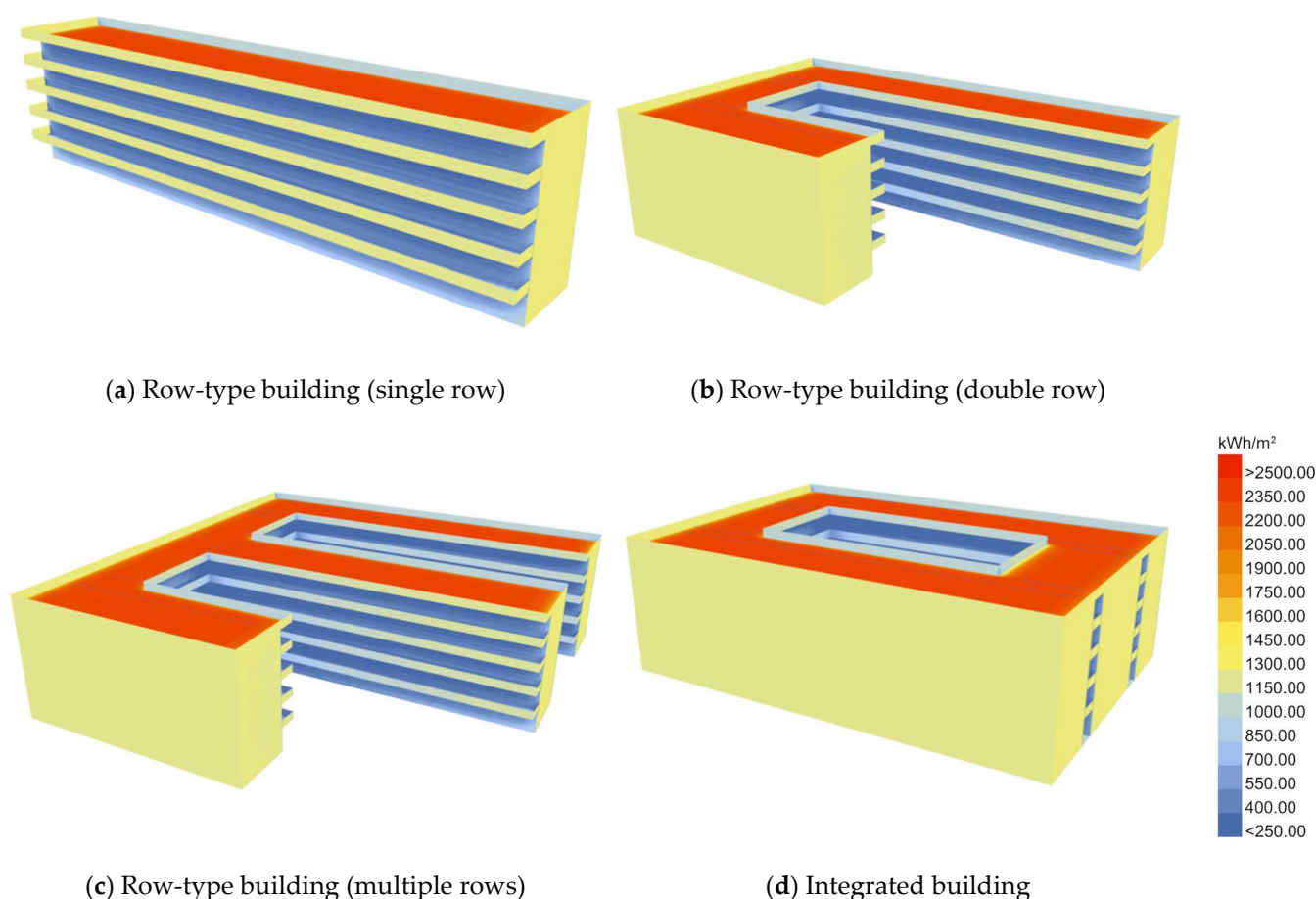


Figure 10. 3D model of annual solar radiation on the exterior of different building types.

Figure 10 shows the solar radiation levels on the surface of four building types. The reflectance by the building surface materials was not considered. The average solar radiation on the roof was 2.2 MWh/m^2 , and that on the walls of the buildings facing east and west was 1.38 MWh/m^2 . The south facade had slightly lower solar radiation than the eastern and western walls, with an average solar radiation of 1.23 MWh/m^2 . The roofs, the southern walls, and the east and west gable walls of the four building types met the standard requirements for solar power generation. Only some of the railing in the south-facing corridor met the requirements. Therefore, the priority for installing photovoltaic systems in primary and secondary schools in Hainan Province is as follows: south-facing roof $>$ eastern and western facades $>$ south facade.

In summary, the four high school building types in Hainan Province have sufficient solar radiation conditions for installing photovoltaic systems. The roof and the east and west walls of primary and secondary school buildings are the most suitable locations for photovoltaic systems to achieve zero-energy consumption.

4.4. Technical Potential of the Photovoltaic System

The technological potential of the photovoltaic system should be analyzed from several aspects: the optimal installation angle and azimuth angle of the photovoltaic modules and the optimal spacing between the front and rear photovoltaic arrays. Efficient rooftop and suitable facade photovoltaic modules must be used to maximize the energy conversion efficiency of the building surface area. This study chose monocrystalline silicon photovoltaic modules (Jingke) for the secondary school in Wanning City. For the facade,

this study used FLEX-03M-1.7M-210W thin-film photovoltaic panels with a dimension (height \times width \times thickness) of 1710 \times 973 \times 17 mm, peak power of 210 W under standard test conditions, and a module efficiency of 14.9%.

4.4.1. Optimization of Photovoltaic Systems

Most teaching buildings of primary and secondary schools in Hainan Province have flat roofs. HVAC equipment and rooftop staircases affect the photovoltaic system's utilization rate. The typical utilization rate of photovoltaic systems on roofs is 0.6–0.95, with an average of 0.6. The conversion coefficient between the installed capacity of rooftop photovoltaics and the available area is approximately 116.7 W/m², and the specific installed capacity is determined based on the array layout. Therefore, this rate was used in this study. For the facade photovoltaics, this study considered that Hainan Province has a relatively low latitude and a relatively large sunlight angle throughout the year. The shading between buildings has a relatively small impact, but the greenery in front of the buildings is relatively lush. Therefore, this study chose to install a facade photovoltaic system on the third floor and higher to avoid the influence of shading. The standard GB50099-2011 "Design Code for Primary and Secondary Schools" requires that the minimum window-to-ground ratio of classrooms in primary and secondary schools is 0.2. The proportion of the usable area for the facade photovoltaic system on different walls (excluding windows) is listed in Table 6.

Table 6. Proportion of useable area for the facade photovoltaic system on different walls of different building types.

Building Type	Building Parts	Proportion of Available Area
Row-type building (single row)	South-facing railing	80%
	Gable on the east	62%
	Gable on the west	62%
Row-type building (double row)	South wall	46%
	Gable on the east	62%
	Gable on the west	54%
Row-type building (multiple rows)	South wall	46%
	Gable on the east	62%
	Gable on the west	51%
Integrated building	South wall	44%
	Gable on the east	56%
	Gable on the west	56%

The optimal tilt angle to maximize solar energy production depends on the latitude. This study considered angles of 0° to 40°, with an increment of 5°. Hainan Province is located at the southernmost point of China and receives direct sunlight on north-facing walls. Therefore, azimuths from 0° to 360° with an increment of 45° were considered.

4.4.2. The Optimal Installation Angle and Azimuth of Photovoltaic Modules

This study used meteorological data from Haikou City to conduct a simulation to optimize the angle and azimuth. The optimal inclination angle to optimize the annual power generation is 15°. Since this study considered schools in the major cities in Hainan Province, this study used a maximum inclination angle for the rooftop photovoltaics of 20°. A smaller inclination angle reduces the visibility of the rooftop photovoltaics. The optimal orientation angle for rooftop photovoltaics in Hainan Province is 0° (due south). The optimal azimuth angles for facade photovoltaics are 90° and 270°. The simulation results showed that the optimal azimuth angles for the facade photovoltaics were 70° and 290°, i.e., 20° southeast and 20° southwest.

4.4.3. The Optimal Installation Angle and Azimuth of Photovoltaic Modules

The standard “Code for Design of Photovoltaic Power Stations” [37] requires a minimum distance for fixed photovoltaic arrays so that they are unobstructed from 9:00 to 15:00 solar time on the winter solstice day.

The minimum spacing between the front and rear photovoltaic arrays can be calculated as follows:

$$D = L \cos \beta + L \sin \beta \frac{0.707 \tan \phi + 0.4338}{0.707 - 0.4338 \tan \phi} \quad (2)$$

where L is the length of the inclined plane of the array, m; D is the distance between two rows of arrays, m; β is the inclination angle of the array, °; ϕ is the local latitude, °.

The optimal minimum spacing between the front and rear rooftop photovoltaic arrays in Hainan Province is 3.1 m, the recommended value nationwide. The relatively small spacing between the front and rear arrays enables the installation of more photovoltaic arrays in the same installation area.

4.5. The Potential of the Production-Demand Balance of the Photovoltaic System

Under typical meteorological year conditions, the annual power generation capacity of the photovoltaic systems of the row-type building (single row), row-type building (double row), row-type building (multiple rows), and integrated building is 116.27 MWh, 194.41 MWh, 311.76 MWh, and 263.96 MWh, respectively.

The row-type building (single row), row-type building (double row), row-type building (multiple rows), and integrated building have areas of 2974 m², 4762 m², 7983 m², and 6301 m² and an average annual energy consumption of 90.41 MWh, 144.77 MWh, 242.68 MWh, and 191.55 MWh, respectively (Figure 11).

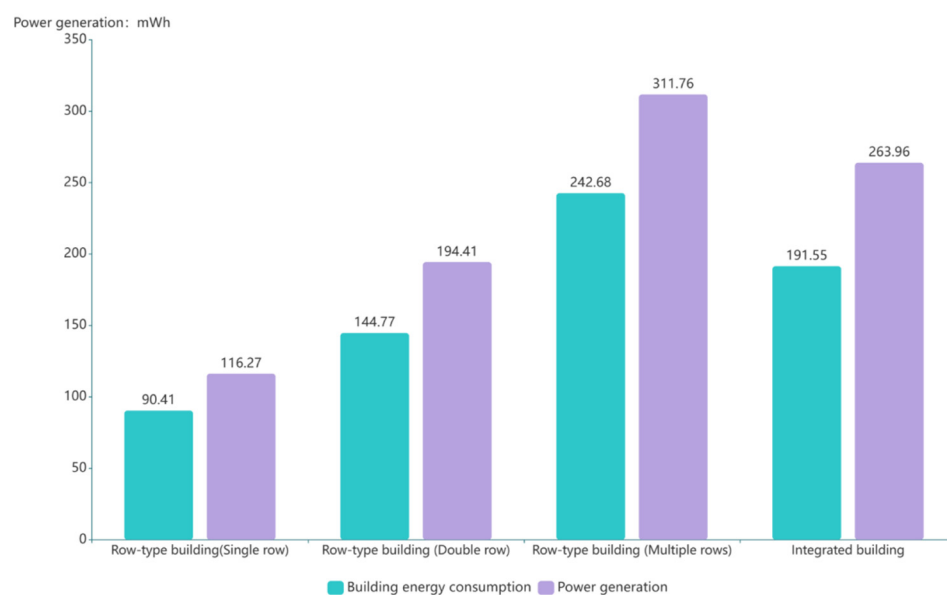


Figure 11. Comparison of the energy consumption and power generation capacity of the photovoltaic system for different building types.

The annual power generation capacity of the four building types exceeds their annual average energy consumption, demonstrating that optimizing the design of building photovoltaic systems can achieve a balance between energy production and demand.

4.6. Economic Potential of the Photovoltaic System

The installed capacity and cost of the rooftop and facade photovoltaic systems for the four building types are listed in Table 7. The initial investment for the rooftop photovoltaic system is \$0.52/Wp. The initial investment in facade photovoltaic systems is relatively high

due to the lack of market scale and high labor and manufacturing costs. A literature review shows that the initial investment cost of a facade photovoltaic system is \$370.35/m² [38].

Table 7. Capacity and cost of roof and facade photovoltaic systems for four building types.

Project	Row-Type Building (Single Row)	Row-Type Building (Double Row)	Row-Type Building (Multiple Rows)	Integrated Building
Installed capacity of photovoltaic system/kWp	69.1	110	189	147
Area of facade photovoltaic system/m ²	192	288	434	340
Investment cost of rooftop photovoltaic system/dollars	36,025.11	57,348.22	98,534.67	76,638.07
Investment cost of facade photovoltaic system/dollars	71,106.65	106,660.04	160,730.72	125,918.06
Total cost/dollars	107,131.75	164,008.26	259,265.39	202,556.13

The dynamic payback period for the four building types is 15.02, 14.45, 13.56, and 13.36 years, respectively, which is significantly higher than for rooftop photovoltaic systems. The integrated building has the highest economic efficiency, followed by the row-type building (multiple rows), row-type building (double row), and row-type building (single row).

The high cost and low photoelectric conversion efficiency of facade thin-film photovoltaics result in lower economic efficiency than rooftop photovoltaics. Due to the high solar radiation intensity on the east and west facades in Hainan Province, integrated buildings with larger east and west wall areas have higher economic efficiency than row-type buildings. Installing photovoltaic systems in newly built schools in high-density cities has excellent economic benefits.

4.7. Environmental Potential of the Photovoltaic System

The total power generation capacity of the photovoltaic systems for four building types over a 25-year life cycle is 2308.05 MWh, 3694.23 MWh, 6187.08 MWh, and 4884.95 MWh, saving 698.19, 117.50, 1871.59, and 1477.70 tons of standard coal throughout the life cycle, as shown in Table 8.

Table 8. Emission reduction of pollutants and total environmental benefits of photovoltaic systems for four building types.

Building Type	Pollutant	Emission Reduction/t	Environmental Benefit/dollars
Row-type building (single row)	CO ₂	1208.57	3864.51
	SO ₂	15.36	12,812.78
	NO _x	6.98	7765.32
	TSP	11.87	3630.29
	Total	1242.78	28,072.91
Row-type building (double row)	CO ₂	1934.39	6185.41
	SO ₂	24.59	20,507.72
	NO _x	11.18	12,428.92
	TSP	19.00	5810.52
	Total	1989.15	44,932.57
Row-type building (multiple rows)	CO ₂	3239.72	10,359.33
	SO ₂	41.18	34,346.35
	NO _x	18.72	20,815.97
	TSP	31.82	9731.47
	Total	3331.43	75,253.12
Integrated building	CO ₂	2557.90	8179.13
	SO ₂	32.51	27,117.91
	NO _x	14.78	16,435.10
	TSP	25.12	7683.41
	Total	2630.31	59,415.55

The pollutant emission reductions of the photovoltaic systems for the four building types compared to coal-fired thermal power generation are 1242.78 tons, 1989.15 tons, 3331.43 tons, and 2630.31 tons. This study divided the total environmental benefits by the total power generation, and the environmental benefits brought by the photovoltaic system in primary and secondary schools in Hainan Province are \$0.012 dollars/kWh.

5. Conclusions

Firstly, the performance of an operational rooftop PV plant in two school buildings is presented in terms of production-demand balance and economic and environmental aspects. Secondly, a comparison of the measured and simulated power generation capacity for a particular site is carried out as a software validation exercise. Finally, the physical, technological, production-demand balance, economic, and environmental related potential of PV in the context of school buildings is assessed for four different building types. The conclusion is as follows:

The teaching buildings in the primary and secondary schools in Hainan Province receive abundant solar radiation suitable for photovoltaic power generation. This part of southern China is rich in solar resources, making it suitable for building photovoltaics. The development of building photovoltaics is relatively mature in the western and central regions of China. The southern region will likely become a key area for developing and implementing building photovoltaics in the future and reducing CO₂ emissions.

Due to Hainan's location at a relatively low latitude, the inclination angle of the photovoltaic modules is smaller than 20°, reducing the visibility of rooftop photovoltaics. The relatively small spacing between the front and rear arrays allows for the installation of a sufficient number of photovoltaic arrays. China has a high density of urban buildings, and roofs are the primary location for installing building photovoltaic systems. The smaller installation angle gives South China and low-latitude countries an advantage in the installed capacity, attracting investors and promoting the installation of building photovoltaic systems.

All four building types achieve balances in energy production and the demand of the photovoltaic systems. Row-type buildings have larger areas for facade photovoltaics, but the systems can only be installed on the east and west facades of the third floors and above to prevent shading. Thus, photovoltaic systems can achieve zero carbon emissions in primary and secondary school buildings. The results provide data support for the zero carbon transformation of primary and secondary school buildings in southern China and other low-latitude countries and information for reducing the carbon emissions of other buildings.

The dynamic investment payback periods for the photovoltaic systems of the four building types are 15.02, 14.45, 13.56, and 13.36 years. The investment cost of building photovoltaics is relatively high, but long-term benefits are achieved. After the investment cost has been recovered, high economic benefits are obtained during the system's lifespan. As the industry rebounds, the investment costs will decrease, and building photovoltaics will provide excellent economic benefits, attracting investors and ensuring government promotion and support. The pollutant emission reductions of the photovoltaic systems for the four building types compared to coal-fired thermal power generation are 698.19 tons, 117.50 tons, 1871.59 tons, and 1477.70 tons throughout the building's life cycles. The environmental benefits of the photovoltaic system in primary and secondary schools in Hainan Province are \$0.012/kWh. The Chinese government will focus increasingly on photovoltaic systems in future urban renewal to reduce carbon emissions.

Our results indicate that installing photovoltaic systems in primary and secondary school buildings can achieve zero carbon emissions, reducing the pressure on urban power grids during holidays. The results are applicable to other types of buildings to ensure that China achieves the carbon peak and carbon neutrality goals.

This study only assessed the potential of photovoltaic systems on the roofs and facades of primary and secondary school buildings, but did not consider other photovoltaic

components, such as photovoltaic windows, louvers, and railings. Therefore, future studies should investigate the application potential of these components. In addition, this study did not consider the hourly difference between photovoltaic power generation capacity and building electricity consumption, but focused on the annual supply-demand balance. Future studies should consider this to improve the accuracy of the results.

Author Contributions: Investigation, F.J.; Data curation, W.C.; Writing—original draft, X.Z. (Xudong Zhang); Writing—review & editing, C.W. and X.Z. (Xiaogang Zhao); Visualization, X.Z. (Xiaogang Zhao). All authors have read and agreed to the published version of the manuscript.

Funding: This research was funded by International Energy Foundation grant number G-2109-33434.

Data Availability Statement: The data is designed to be used in other ongoing research and should be protected before official publication.

Conflicts of Interest: Author Wang Chen was employed by the company Tropical Building Science Research Institute (Hainan) Co., Ltd. The remaining authors declare that the research was conducted in the absence of any commercial or financial relationships that could be construed as a potential conflict of interest.

References

1. Zhang, H.; Wang, L.X.; Li, Z. Evaluation method and application of photovoltaic potential of urban building roof. *Urb. Probl.* **2017**, *36*, 33–39. [[CrossRef](#)]
2. Hu, M.J.; Liu, Z.; Huang, Y.H.; Wei, M.J.; Yuan, B. Estimation of Rooftop Solar Photovoltaic Potential Based on High-Resolution Images and Digital Surface Models. *Buildings* **2023**, *13*, 2686. [[CrossRef](#)]
3. Ranjgar, B.; Niccolai, A. Large-Scale Rooftop Solar Photovoltaic Power Production Potential Assessment: A Case Study for Tehran Metropolitan Area. Iran. *Energies* **2023**, *16*, 7111. [[CrossRef](#)]
4. Zhao, K.M.; Gou, Z.H. Influence of urban morphology on facade solar potential in mixed-use neighborhoods: Block prototypes and design benchmark. *Energy Build.* **2023**, *297*, 113446. [[CrossRef](#)]
5. Singh, D.; Gautam, A.K.; Chaudhary, R. Potential and performance estimation of free-standing and building integrated photovoltaic technologies for different climatic zones of India. *Energy Built Environ.* **2022**, *3*, 40–55. [[CrossRef](#)]
6. Singh, D.; Chaudhary, R.; Karthick, A. Review on the progress of building-applied/integrated photovoltaic system. *Environ. Sci. Pollut. Res.* **2021**, *28*, 47689–47724. [[CrossRef](#)]
7. Chandrika, V.; Thalib, M.M.; Karthick, A.; Sathyamurthy, R.; Manokar, A.M.; Subramaniam, U.; Stalin, B. Performance assessment of free standing and building integrated grid connected photovoltaic system for southern part of India. *Build. Serv. Eng. Res. Technol.* **2021**, *42*, 237–248. [[CrossRef](#)]
8. Zhang, W.J.; Huang, F.C.; Mao, K.; Lin, C.Q.; Pan, Z. Evaluation of Photovoltaic Energy Saving Potential and Investment Value of Urban Buildings in China Based on GIS Technology. *Buildings* **2021**, *11*, 649. [[CrossRef](#)]
9. Wang, Y.; Jiang, P.P. Research on solar photovoltaic transformation potential of existing residential areas in Shanghai. *Hous. Sci.* **2021**, *41*, 48–54. [[CrossRef](#)]
10. Chen, Y.B.; Tan, H.W.; Li, S.M.; Song, X.D. GIS-based dimensionless assessment of distributed rooftop PV in Chinese residential communities. *Procedia Eng.* **2017**, *205*, 205–212. [[CrossRef](#)]
11. Xu, W.; Zhang, H.H. Solar energy utilization potential evaluation of public building photovoltaic system. *J. Chongqing Univ.* **2021**, *44*, 53–62. [[CrossRef](#)]
12. Liu, C.P.; Xu, W.; Zou, Y. Analysis of photovoltaic potential in different climate regions of China. *Build. Sci.* **2019**, *35*, 1–7+15.
13. Wiginton, L.K.; Nguyen, H.T.; Pearce, J.M. Quantifying rooftop solar photovoltaic potential for regional renewable energy policy. *Environ. Urb. Syst.* **2010**, *34*, 345–357. [[CrossRef](#)]
14. Izquierdo, S.; Rodrigues, M.; Fueyo, N. A method for estimating the geographical distribution of the available roof surface area for large-scale photovoltaic energy-potential evaluations. *Sol. Energy* **2008**, *82*, 929–939. [[CrossRef](#)]
15. Feng, S.J.; Li, S.M. Analysis of Building Application Potential of Solar Energy Resources in Panzhihua Area. *Sichuan Archit.* **2016**, *36*, 84–86, 88. [[CrossRef](#)]
16. Jacques, D.A.; Gooding, J.; Giesekam, J.J.; Tomlin, A.S.; Crook, R. Methodology for the assessment of PV capacity over a city region using low-resolution LiDAR data and application to the City of Leeds (UK). *Appl. Energy* **2014**, *124*, 28–34. [[CrossRef](#)]
17. Khan, J.; Arsalan, M.H. Estimation of rooftop solar photovoltaic potential using geo-spatial techniques: A perspective from planned neighborhood of Karachi–Pakistan. *Renew. Energy* **2016**, *90*, 188–203. [[CrossRef](#)]
18. Wang, G.H.; Tang, X.M.; Zhang, T.; Dai, H.L.; Peng, Y.Y. Potential analysis of national building remote sensing monitoring and distributed photovoltaic construction. *Chin. Eng. Sci.* **2021**, *23*, 92–100. [[CrossRef](#)]
19. Mekhilef, S.; Saidur, R.; Kamalisarvestani, M. Effect of dust, humidity and air velocity on efficiency of photovoltaic cells. *Renew. Sustain. Energy Rev.* **2012**, *16*, 2920–2925. [[CrossRef](#)]

20. Liu, Z.D.; Zhang, S.D.; Jia, H. Economic and Environmental Benefit Analysis of Grid Connected Photovoltaic Systems in Anyang City. *Chin. Electr. Power* **2013**, *46*, 43–47. [CrossRef]
21. Brito, M.C.; Freitas, S.; Guimarães, S.; Catita, C.; Redweik, P. The importance of facades for the solar PV potential of a Mediterranean city using LiDAR data. *Renew. Energy* **2017**, *111*, 85–94. [CrossRef]
22. Gong, X.L.; Jiang, W.; Qian, S.H. Development Potential and Benefit Analysis of Rural Household Photovoltaic Power Generation. *Agric. Sci. Technol. Equip.* **2015**, *37*, 49–50. [CrossRef]
23. Liu, J.J.; Gao, L.C.; Zhang, X.P.; Hao, Q.Y.; Xie, Y. Economic analysis of distributed photovoltaic power generation technology based on EPC mode. *Henan Sci.* **2021**, *39*, 1738–1745. [CrossRef]
24. Peng, J.Q.; Lin, L. Investigation on the development potential of rooftop PV system in Hong Kong and its environmental benefits. *Renew. Sustain. Energy Rev.* **2013**, *27*, 149–162. [CrossRef]
25. Zhang, M.; Liu, J.; Lin, J.G.; Zhao, X.B. Environmental benefit analysis of rooftop distributed photovoltaic development under the background of “dual carbon”. *Energy Res. Utiliz.* **2021**, *33*, 37–41.
26. Zhao, T.X.; Liao, H.; Li, J.T.; Yin, J.C.; Jing, M.M.; Ma, X.; Liu, Z.M. Economic and Environmental Benefit Analysis of BIPV—Taking Yunnan Normal University’s 120kWp Photovoltaic Curtain Wall as an Example. *Sol. Energy* **2017**, *38*, 62–65, 61.
27. 11th Province Shanxi Province Issued the Policy of Promoting Distributed Photovoltaic in the Whole County (Report before 9 July). Available online: <https://baijiahao.baidu.com/s?id=1703804914999411688&wfr=spider&for=pc> (accessed on 30 July 2021).
28. Zhang, R.; Liu, C.P.; Du, X.; Li, G.H.; Chen, W. Research on the Potential of Photovoltaic Application in Existing Buildings in Hainan Province Based on Typical Case Analysis. *Constr. Technol.* **2022**, *21*, 36–40. [CrossRef]
29. DB 46/T481-2019; Energy Consumption Quota Standard for Public Institutions in Hainan Province. Hainan Provincial Administration for Market Regulation: Haikou, China, 2019.
30. Notice of Hainan Provincial Development and Reform Commission on Forwarding the Notice of the National Development and Reform Commission on Further Deepening the Market-Oriented Reform of Coal-Fired Power Generation Grid Electricity Prices. Available online: <https://www.hainan.gov.cn/data/zfgb/2022/05/9689> (accessed on 20 October 2021).
31. Zhu, Q.Z.; Si, L.L.; Jiang, T.Y. Economic and Environmental Benefits of Building Photovoltaic Systems with Different Installation Methods. *J. Sol. Energy* **2012**, *33*, 24–29. [CrossRef]
32. Sun, Y.W.; Wang, R.; Xiao, L.S.; Liu, J.; Yu, Y.J.; Zhuang, X.S. Economic and environmental benefits of China’s grid connected photovoltaic power generation system. *Chin. Popul. Resour. Environ.* **2011**, *21*, 88–94. [CrossRef]
33. Wei, X.H.; Zhou, H. Estimation of Environmental Value Standards for Reducing Pollutants in China’s Thermal Power Generation Industry. *Environ. Sci. Res.* **2003**, *16*, 53–56. [CrossRef]
34. GB 50099-2011; Code for Design of School. General Administration of Quality Supervision, Inspection and Quarantine of the People’s Republic of China: Beijing, China, 2010.
35. Compagnon, R. Solar and daylight availability in the urban fabric. *Pop. Utiliz. Electr.* **2004**, *36*, 321–328. [CrossRef]
36. Yin, H.M.; Zhang, L.Z. Design of universities apartments in Jinan based on solar energy utilization potential. *J. Shandong Jianzhu Univ.* **2020**, *35*, 46–52. [CrossRef]
37. GB 50797-2012; Code for Design of Photovoltaic Power Station. General Administration of Quality Supervision, Inspection and Quarantine of the People’s Republic of China: Beijing, China, 2012.
38. Jiang, K.; Gu, F.Y.; Li, X.; Wang, L. Economic analysis of copper indium gallium selenium photovoltaic curtain wall technology. *J. Archit.* **2019**, *S2*, 92–95.

Disclaimer/Publisher’s Note: The statements, opinions and data contained in all publications are solely those of the individual author(s) and contributor(s) and not of MDPI and/or the editor(s). MDPI and/or the editor(s) disclaim responsibility for any injury to people or property resulting from any ideas, methods, instructions or products referred to in the content.